Available online at www.sciencedirect.com
ScienceDirect
Nuclear Instruments and Methods in Physics Research A 577 (2007) 215–222
NUCLEAR INSTRUMENTS & METHODS IN PHYSICS RESEARCH Section A
www.elsevier.com/locate/nima

Plans for longitudinal and transverse neutralized beam compression experiments, and initial results from solenoid transport experiments

P.A. Seidl[a,*], J. Armijo[a,g], D. Baca[a], F.M. Bieniosek[a], J. Coleman[a,f], R.C. Davidson[d], P.C. Efthimion[d], A. Friedman[b], E.P. Gilson[d], D. Grote[b], I. Haber[c], E. Henestroza[a], I. Kaganovich[d], M. Leitner[a], B.G. Logan[a], A.W. Molvik[b], D.V. Rose[e], P.K. Roy[a], A.B. Sefkow[d], W.M. Sharp[b], J.L. Vay[a], W.L. Waldron[a], D.R. Welch[e], S.S. Yu[a]

[a]*Lawrence Berkeley National Laboratory, Berkeley, CA 94720, USA*
[b]*Lawrence Livermore National Laboratory, Livermore, CA 94550, USA*
[c]*University of Maryland, College Park, MD 20742-3511, USA*
[d]*Princeton Plasma Physics Laboratory, Princeton, NJ 08543-0451, USA*
[e]*Voss Scientific, Albuquerque, NM 87108, USA*
[f]*University of California, Berkeley, CA 94720, USA*
[g]*École Normale Supérieure, Paris Cedex 05, France*

Available online 22 February 2007

Abstract

This paper presents plans for neutralized drift compression experiments, precursors to future target heating experiments. The target-physics objective is to study warm dense matter (WDM) using short-duration (~1 ns) ion beams that enter the targets at energies just above that at which dE/dx is maximal. High intensity on target is to be achieved by a combination of longitudinal compression and transverse focusing. This work will build upon recent success in longitudinal compression, where the ion beam was compressed lengthwise by a factor of more than 50 by first applying a linear head-to-tail velocity tilt to the beam, and then allowing the beam to drift through a dense, neutralizing background plasma. Studies on a novel pulse line ion accelerator were also carried out. It is planned to demonstrate simultaneous transverse focusing and longitudinal compression in a series of future experiments, thereby achieving conditions suitable for future WDM target experiments.

Future experiments may use solenoids for transverse focusing of un-neutralized ion beams during acceleration. Recent results are reported in the transport of a high-perveance heavy ion beam in a solenoid transport channel. The principal objectives of this solenoid transport experiment are to match and transport a space-charge-dominated ion beam, and to study associated electron-cloud and gas effects that may limit the beam quality in a solenoid transport system. Ideally, the beam will establish a Brillouin-flow condition (rotation at one-half the cyclotron frequency). Other mechanisms that potentially degrade beam quality are being studied, such as focusing-field aberrations, beam halo, and separation of lattice focusing elements.
© 2007 Elsevier B.V. All rights reserved.

PACS: 29.17.+w; 41.75.Ak; 52.65.Rr

Keywords: Neutralized drift compression; Charged-particle beams; Particle-in-cell simulations; Beam–plasma interaction

1. Introduction

Accelerators producing intense beams of heavy ions can create uniformly heated matter. They can enable the study of strongly coupled plasma physics in the warm dense matter (WDM) regime in the near term, and the study of other high-energy density physics regimes afterward. The WDM regime (at densities of ~0.01–10 times solid density, and temperatures of ~0.1–10 eV) is characterized by the space-charge potential energy of neighboring ions being of the same order as or greater than the ion thermal energy, so that the traditional "weak-coupling" theory of ordinary plasmas breaks down, and theoretical descriptions become

*Corresponding author. Tel.: +1 510 486 7653; fax: +1 510 486 5392.
E-mail address: PASeidl@lbl.gov (P.A. Seidl).

0168-9002/$ - see front matter © 2007 Elsevier B.V. All rights reserved.
doi:10.1016/j.nima.2007.02.055

more complex. The physics applications of heavy ion beams require understanding the fundamental physics limits to the compression of ion beams in both space and time before they reach the target, as well as a basic understanding of collective beam–plasma interaction processes and beam energy deposition profiles within the dense plasma targets. The ions slow down with minimal side-scattering, and their rate of energy loss has a pronounced (Bragg) peak, the magnitude of which increases with the beam ion charge state. These properties make heavy ions an excellent driver for high-energy density physics studies, wherein thin targets would be uniformly heated by locating the deposition peak near the target center. The primary scientific challenge in exploiting these desirable properties in the creation of high energy density matter and fusion ignition conditions in the laboratory is to compress the beam in time ($\sim 10^2\times$ for WDM studies, higher for inertial fusion energy application) to a pulse length that is short compared to the target disassembly time, while also compressing the beam in the transverse direction (radial $\sim 10\times$) to a small focal spot, yielding a region of matter at high-energy density. Near-term experiments are described in Refs. [1,2].

The high space-charge force of the intense ion beams limits the compression. Compressing the ion beam within neutralizing plasma allows significantly higher beam line charge densities, extending the allowed beam parameter space into high-intensity regimes where it would not otherwise propagate. Beam–plasma collective effects in these regimes (including an environment of longitudinal and transverse magnetic fields) have been explored to some extent, but more work remains. A basic understanding of the collective processes and nonlinear dynamics of intense, high-brightness, heavy ion beams, and a determination of how best to create, accelerate, transport, compress, and focus these beams to a small spot size and short pulse length are critical to achieving the scientific objectives of ion-beam-driven studies of warm dense matter and of heavy ion fusion.

This paper focuses on the plans and recent results of beam dynamics experiments toward the high-intensity conditions suitable for WDM studies. In order to provide the needed target energy deposition ($\approx 10\,\mathrm{kJ/g}$), a short pulse ($\sim 1\,\mathrm{ns}$) and high line charge density beam focused onto a thin target must be produced. Aluminum foam (10% of solid density) is a typical target considered. The key accelerator components envisioned are a high-current, high-brightness ion source; a short-pulse injector; an accelerator section with focusing elements for high line charge density transport; a neutralized drift compression section to provide longitudinal compression of the intense ion beam, enabled by a neutralizing plasma; and a final focus using a high field solenoid to compress the beam transversely, also neutralized with a background plasma. For the high line-charge density beam transport, we have commenced experiments and modeling with solenoids, which are well suited to low-energy and high-current ion beams. While solenoids are commonplace in electron induction machines, the experimental experience with ion beams is limited.

All these components, except for the high-field solenoid, have been studied in recent experiments. They are described below, along with our plans for the future. Section 2 describes the experimental apparatus and summarizes the results to date of neutralized drift compression. Section 3 summarizes beam tests of a slow-traveling wave structure for ion acceleration, the pulse line ion accelerator (PLIA), an alternative to the base-line technique of induction acceleration. Section 4 describes the planned simultaneous longitudinal compression and transverse focusing experiments aimed at validating the components of a future WDM target heating facility. Section 5 summarizes recent results from a solenoid transport experiment.

2. Neutralized drift compression experiment setup

The neutralized drift compression experiment (NDCX) facility began operation in December 2004. The description in this section pertains to the setup for drift compression experiments from December 2004 to July 2005 except where indicated otherwise.

A non-relativistic K^+ ion beam is given a head-to-tail velocity ramp using an induction bunching module, and then allowed to compress axially while drifting through a pre-formed plasma column. Neutralized drift compression simulations show that the minimum compressed pulse duration is limited only by the accuracy of the applied velocity tilt and the longitudinal velocity spread of the beam, as long as the background plasma density greatly exceeds the ion beam density throughout the drift region and the background plasma is cold enough. The induction bunching module adds a linear velocity ramp from the head to the tail of a selected 250–500 ns portion of the 23–26 mA, 280–310 keV NDCX beam. The ramp is applied with an induction drive pulse of $-80\,\mathrm{kV} < \Delta V < +70\,\mathrm{kV}$ amplitude. The rear of the ramped beam section catches up with the head in a 1 m drift section that is pre-filled with plasma confined in a weak solenoid magnetic field. The drift compression section provides space-charge neutralization during axial compression. Four matching quadrupole magnets control the beam envelope conditions at the entrance to the bunching module. The beam current and transverse beam distribution near the point of maximum compression were measured with a variety of diagnostics, with and without the application of the velocity tilt. A compression ratio, $R = I_{\max}(\mathrm{bunched})/I_o \geqslant 50$, was observed. The results [3,4] are compared to simulations in Ref. [5], along with parametric variations of the beam energy and bunching module waveform. Radial focusing in neutralizing plasma was demonstrated earlier in Ref. [6].

The beam diagnostics included slit scanners and scintillators for the measurement of the transverse beam phase space just upstream of the bunching module, and a scintillator and gated CCD camera for measuring the

transverse current density distribution near the focal plane at the exit of the drift compression section. Near the focal plane, the development of a fast "pinhole" Faraday cup with ~1 ns response time was required to resolve the compressed beam current pulse whose duration was a few nanoseconds [5]. The Faraday cup entrance had multiple small apertures to prevent the neutralizing plasma from reaching the ion collector and confounding the results. A scintillator and photomultiplier tube were a complementary method to measure the time dependence of the compressed beam current pulse.

Two cathodic-arc plasma sources (CAPS) [7], located after the downstream end of drift compression column (and therefore close to the beam focal spot), were used in these experiments to inject plasma into the drift compression region after the bunching module. The drift compression section was surrounded by a weak (~0.02 T) magnetic field which helped confine and direct the plasma to the upstream end of the drift section, where a dipole field prevented back-streaming plasma from entering the bunching module gap. Based on magnetic field and plasma transport modeling, the plasma density achieved to date, $n_p \approx 5 \times 10^{10}\,\mathrm{cm}^{-3}$, can probably be increased significantly by optimizing the geometry of the plasma sources with respect to the drift column.

Recently, a new approach to fill the drift section with neutralizing plasma from discharges on the inner surface of a ceramic-lined drift column has been pursued. In preliminary tests [8], the barium titanate ferro-electric plasma source produces a plasma density $n_p = 2\text{–}8 \times 10^{10}/\mathrm{cm}^3$, similar to that of the CAPS source. Looking ahead to WDM target heating experiments, the extra space near the focal spot is attractive (no CAPS sources are needed).

Both these methods of neutralizing the beam will be tested in upcoming transverse focusing and longitudinal compression experiments.

From August 2005 to December 2005, beam tests with a constant energy beam (no velocity tilt from the induction bunching module) injected into a prototype PLIA were carried out along with commissioning of and measurements with a newly constructed electrostatic energy analyzer. Those results are summarized in Section 3.

In January 2006, the matching quadrupoles, PLIA and energy analyzer were replaced with two solenoids. Results from measurements of beam transport through two solenoids are described in Section 5. Four solenoid transport experiments are underway now. Following the solenoid transport experiments, the induction bunching module, and energy analyzer will be added to the setup for further drift compression experiments described in Section 4.

3. Pulse line ion accelerator

The PLIA is a helical coil structure (Fig. 1a), submerged in a dielectric medium (oil) and powered by a pulsed high-voltage waveform to impart beam energy gains many times higher than the input voltage to the helix. Ions are accelerated in the helical structure by a traveling electric field. The PLIA concept and first experiment results are described in Refs. [9,10], respectively.

Fig. 1(b) is a simplified applied voltage profile on the helix coil. The actual voltage waveform is a damped ringing waveform with a period of 0.7 μs for a few periods. Fig. 1(c) shows the prototype helical structure.

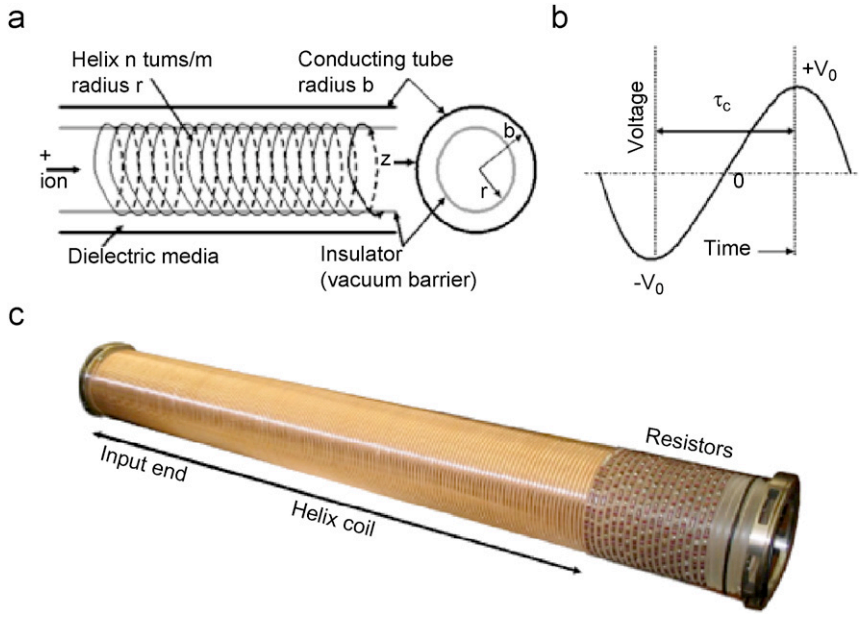

Fig. 1. (a) A schematic of the helical pulse line structure. Helical pulse line of radius r is located inside of a conducting cylinder of radius b, and a dielectric media is located in the region outside the helix. (b) Schematic of a drive voltage waveform applied at the helix input. (c) Mechanically constructed helix for the PLIA experiments.

For an incoming, nearly monochromatic beam of $E = 0.35\,\mathrm{MeV}$, the PLIA modulated the beam energy in the range $-80\,\mathrm{keV} \leqslant \Delta E \leqslant +150\,\mathrm{keV}$ for an applied voltage pulse of maximum range -21 to $+12\,\mathrm{kV}$. K^+ ions were both accelerated and decelerated because the incoming beam bunch was $>10\,\mu\mathrm{s}$ long, spanning both accelerating and decelerating components of the traveling wave. This experiment demonstrated the PLIA concept: due to the accelerating field from the traveling wave of the helical slow wave structure, significant energy amplification was achieved with modest voltage pulses.

The PLIA exhibited puzzling flashovers at relatively low voltages. For these experiments, the voltage swing was limited to 33 kV, corresponding to an average ion acceleration gradient of $\approx 150\,\mathrm{kV/m}$. This is well below the $>1\,\mathrm{MeV/m}$ range necessary to make it attractive for future applications, so the problem continues to be investigated via simulations and design modifications [11,12]. When solved, the PLIA concept has the potential to achieve high acceleration gradients at a modest cost. We are performing end-to-end simulations of drivers for WDM experiments, utilizing PLIA modules followed by final neutralized drift compression and focusing. Studies of induction-based WDM drivers are also underway.

4. Simultaneous longitudinal compression and transverse focusing

In the experiments described in Section 2 and in Ref. [3], the beam transverse envelope parameters were not optimized to achieve the minimum focal spot size at the point of maximum axial compression. This is due to the variation of ion kinetic energy through the bunching module gap and the finite radial electric field due to the dual-iris geometry of the gap [13]. Detailed particle-in-cell (PIC) simulations quantified the effect [14]. The simulation shown in Fig. 2 illustrates the anticipated improvement.

The rms beam radius is shown versus time in the bunch at the focal plane. By increasing the convergence angle of the beam from 7.5 to 13.5 mrad at the entrance to the bunching module, the beam radial compression is at a maximum when the current longitudinal compression ratio is $R \approx 50$. Demonstrating simultaneous longitudinal and transverse focusing will be a principal objective of the next round of experiments.

Assuming an ideal waveform and a 0.2 eV beam longitudinal temperature, a significantly higher compression ($R > 100$) would be possible with an induction bunching module capable of a greater voltage swing ($\pm 150\,\mathrm{kV}$) over a longer time duration ($0.7\,\mu\mathrm{s}$), as indicated by PIC simulations [15]. Such an induction module is being constructed. With two (or more) induction modules, it will also be possible to apply a series of energy modulations to the beam (acceleration and/or velocity tilts).

The fidelity of the voltage pulse that applies a linear velocity ramp to the beam limits the achievable compression ratio. In particular, medium-wavelength errors (only a few periods per ramp duration) are most significant. It appears from preliminary parametric sensitivity studies that errors up to $\approx 1\%$ are tolerable. The waveform accuracy of the bunching module is also in this range. High-frequency errors are averaged out over the transit time of ions through the acceleration gap ($\approx 0.05\,\mu\mathrm{s}$), and very low-frequency errors correspond in leading order to a slightly different ramp slope, $\mathrm{d}v/\mathrm{d}t$, where v is the ion velocity. These slope errors, if repeatable, can be easily compensated with minor adjustments to the ion kinetic energy of the injected beam, adjustments to the upstream beam envelope, and by slight changes to the axial position of the diagnostics (or WDM target) at the focal plane.

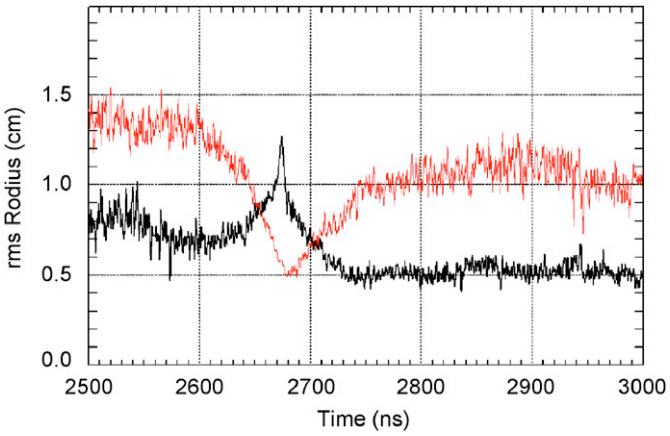

Fig. 2. LSP particle-in-cell simulation of two scenarios of drift compression (black) without and (red) with compensation for the defocusing in the gap of the bunching module.

Another limitation to the compression is the initial longitudinal temperature of the beam. In the injector, the temperature of the ion-emitting surface is about 1100 °C, or 0.1 eV. PIC simulations tend to show accelerative cooling effects due to ion acceleration in the injector, as described in Ref. [16]. The first direct measurements of the NDCX longitudinal energy spread of the coasting beam using the new electrostatic energy analyzer yields $T_{\parallel} \leqslant (\Delta E)^2/(2E) \leqslant 1.5\,\mathrm{eV}$, where ΔE is the energy spread measured in the lab frame and E is the ion kinetic energy. This value is an upper limit due to coarse sampling in these first commissioning measurements with the energy analyzer, and is considerably higher than PIC simulation results. However, $T_{\parallel} \approx 1\,\mathrm{eV}$ is still compatible with the compression ratios observed so far, and with plans for future experiments [14].

The simulation in Fig. 3 illustrates the importance of the neutralizing plasma to achieving high intensity on target. The compression ratio is four-fold greater due to the presence of the plasma.

A strong ($B_z = 3$–$15\,\mathrm{T}$) final focus solenoid has been shown in simulations to increase the integrated beam energy deposition by up to a factor 10, by creating a smaller beam radius at the focal plane. This is presented in more detail in Refs. [14,15]. We will test an existing

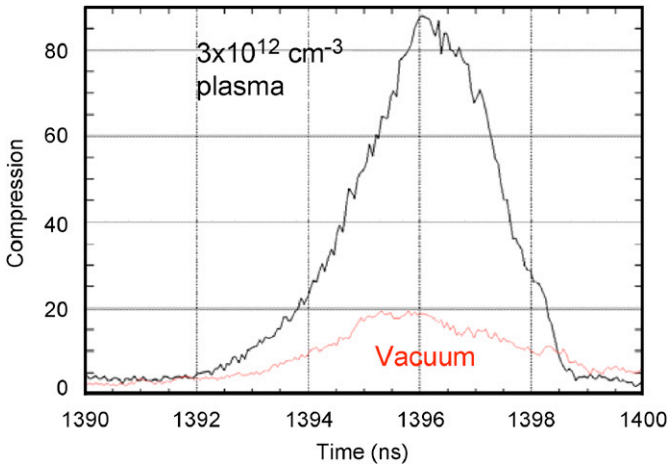

Fig. 3. Simulation of neutralized drift compression with and without the background plasma.

0.5-m-long pulsed solenoid (see Section 5) for operation near 5 T, and carry out experiment design studies with this and higher field magnets. For example, compressing the 0.3 MeV, 45 mA beam with the bunching module, followed by a 15 T solenoid, (0.13-m long) creates $J = 0.55\,\mathrm{J/cm^2}$ on target, and a target temperature of $T_{\mathrm{tgt}} \approx 0.2\,\mathrm{eV}$, within the region of interest for WDM studies. Since 15 T is a rather high field and may present some complications for diagnosing the target, lower field magnets are also being studied. Reducing the field to 5 T reduces the beam density by a factor 2.5 [15].

We are also studying WDM experiments via neutralized drift compression with a 1.6 MeV, 0.36 A K^+ beam using the HCX apparatus [17]. The higher initial kinetic energy and higher beam current, in conjunction with a bunching module, plasma drift compression section and final focusing solenoid, would yield $6.7\,\mathrm{J/cm^2}$ on target, corresponding to $T_{\mathrm{tgt}} \approx 0.6\,\mathrm{eV}$. These values are approximate and based on an ideal bunching module waveform with a voltage swing of 200 kV, and a plasma of sufficiently high density to maintain charge neutrality in the vicinity of the target. The effect of hydrodynamic disassembly during the few ns compressed pulse is also included, and found to decrease the specific energy deposition by 20%.

In some of the modeled situations, the peak beam density at focus can rise above $n_{\mathrm{b}} \approx 10^{14}\,\mathrm{cm^{-3}}$, setting the eventual requirements for neutralizing plasma sources. Furthermore, the injection of sufficiently high plasma into the drift region is complicated by the high magnetic field. Injection from the downstream end of the plasma column and final focus solenoid, where the beam density is greatest appears promising [15].

Because these near-term WDM experiment concepts are based on compressing a section of the longer injected beam, target pre-heat from early-time uncompressed beam must be considered. (Later, we plan to design and build a short-pulse injector that would deliver a beam pulse that is entirely captured and compressed by the bunching module.) If the early time uncompressed beam were to heat and initiate significant hydrodynamic expansion, interpretation of the target physics could be much more difficult. Though more work is necessary to settle the issue definitively, preliminary studies indicate that the early-time uncompressed beam does not deposit much energy in the target due to a larger beam radius. Also, time-dependent focusing techniques are being studied that would further mitigate the pre-heat issue.

5. Solenoid transport experiments—first results

The principal objectives of the solenoid transport experiment are to match and transport a space-charge dominated ion beam, and to study associated electron-cloud and gas effects that may limit the beam quality or beam control in a solenoid transport system. Other mechanisms that would degrade beam quality are being studied, such as focusing-field aberrations, beam halo, and separation of lattice focusing elements.

Two solenoids and a set of diagnostics have been installed on the NDCX beam line. A new alumino-silicate emitter was installed at the beginning of the experiment. Following thorough characterization of the beam after two solenoids, two more solenoids have been added along with diagnostics to study electron cloud and gas effects.

The solenoids are operated at room temperature and in a pulsed mode up to 12 kA (3 T) via SCR-switched capacitive discharge pulsers. The pulse duration is approximately a half-sine wave of 4-ms duration, capable of a repetition rate of 0.07 Hz. The coil lengths range between 43 and 44 cm, with an inner diameter of 10.2 cm. Eighty-two turns in four layers (radial build of the four layers = 3.0 cm) of windings establish the field. There is no iron field-return yoke. In preparation for the experiment and in order to enable accurate modeling, magnetic field probes measured the magnetic field, with particular attention paid to the end regions where the field varies rapidly with position, and also to eddy current effects due to the conducting beam pipe and nearby metal structures. A detailed CAD-based model of the solenoid has been updated based on the field measurements, and will be used to generate a grid of realistic field points for input to PIC simulations. In the fringe of the solenoid, the eddy currents perturb the field by 20–30%. The detailed measurements of the eddy current effects are also well reproduced by a transient model of the solenoid field based on an optimized CAD model including nearby magnetic materials. The integrated focusing strength, $\int B_z^2\,\mathrm{d}z$, of the solenoid is diminished by only a few percent by the eddy currents.

5.1. Characterization of the initial beam distribution

For some of the solenoid experiments, a beam-current limiting aperture has been removed. With the aperture ($r = 1$ cm), the injected beam current is 25 mA. Without the aperture, the current is 45 mA. All measurements reported here are for a beam kinetic energy of 0.3 MeV.

Before installing the solenoids, the initial transverse phase space of the 25-mA beam was measured. The injected beam was previously measured in 2002 prior to installation of the magnetic quadrupoles, and not since that time. Because of beam matching constraints, there was little space for permanent beam diagnostics between the magnetic quadrupoles and the exit of the injector. Thus it was critical to verify the injected beam quality and check for changes due to possible movement of the apparatus and misalignment over time. Since then, the design of the diagnostics and their sensitivity to transverse phase space correlations have improved. Computational methods for reconstructing four-dimensional particle distributions derived from two- and three-dimensional projections of the measured transverse phase space have been developed [18]. The measurements and reconstructed phase space will enable detailed simulations of the beam transport through the solenoids. The measured transverse phase space at the exit of the diode is shown in Fig. 4. The emittance, ($\varepsilon_n = 0.09$ mm mrad for the 45 mA beam at 0.3 MeV, and $\varepsilon_n = 0.06$ mm mrad for the 25 mA beam) and beam current are consistent with the measurements of 2002. The new beam imaging techniques yield more details of the distribution function, which in turn will enable more precise simulations downstream of this measurement point. We have carried out preliminary computational tests using the recent measured data to reconstruct a four-dimensional distribution for PIC simulations, and the results suggest that the measurements are of sufficiently high detail to achieve that goal.

5.2. Solenoid transport

The experimental setup is shown in Fig. 5, with four solenoids. A similar configuration preceded this, with only two solenoids followed by beam intercepting diagnostics. The center-to-center spacing of the solenoids is 60 cm, and can be adjusted for future beam dynamics studies. The diagnostics include slit and Faraday cup scanners and a scintillator. There is a cylindrical electron suppressor, normally biased to −2.5 kV, which suppresses the backstreaming of electrons and low-energy ions generated on or near the intercepting diagnostics. The beam was extracted at 300 kV from the diode and injected into the two solenoids (each with peak axial magnetic fields of $B_1 = B_2 = 2.7$ T). The residual magnetic fields at the diagnostic planes are 0.01–0.1 T, and this, along with the small field near the ion emitter, implies that the beam has a small rotation at the diagnostic plane. The measured beam current (Faraday cup) at the exit is 45 mA, while the WARP PIC model predicts at least 48 mA, with no beam loss through the solenoid system. This discrepancy, due possibly to several effects including Marx voltage calibration and diode geometry details, will be clarified in upcoming measurements and simulations.

The beam current-limiting aperture is located between the exit of the diode and the entrance of the first solenoid magnet. The aperture resides in the fringe field of this first solenoid, which results in additional eddy current effects. When transporting the apertured beam through the solenoid channel, the measured beam current, $I_b = 29$ mA, is greater than the 25 mA measured at the exit of the diode with no solenoids. This is presumably due to the magnetic field focusing a greater fraction of the extracted beam through the aperture. A quantitative explanation will be pursued via PIC simulations using detailed modeling of the magnetic field including the eddy current effects.

Various projections of the transverse phase space distribution, such as $f(x, x', y)$, have also been measured.

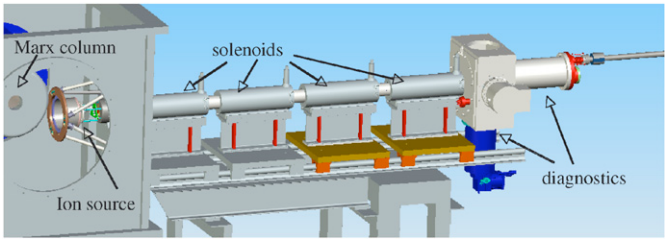

Fig. 5. CAD model of the solenoid transport experiment.

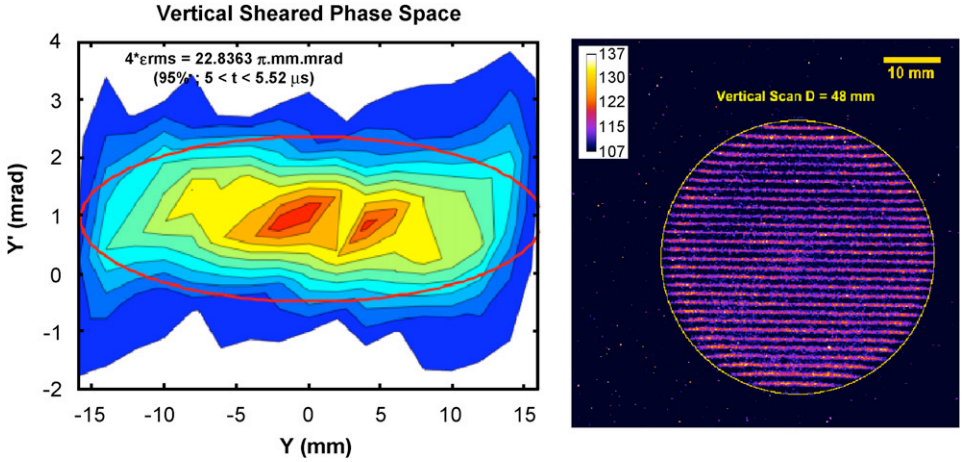

Fig. 4. Vertical (y, y') phase space and the current density distribution $J(x, y)$ of the 45 mA beam.

For the 45 mA beam, the emittance ($\varepsilon_n = 0.09$ mm mrad) is unchanged after two solenoids. The transverse phase space is shown in Fig. 6. The beam centroid trajectory at the diagnostic plane is off center by $\Delta y = -1.3$ mm and $\Delta y' = 7.8$ mrad, due to alignment of the source assembly, diode and magnetic field principle axes with respect to the beamline axis. It is interesting to note that the current density distribution $J(x, y)$ as measured with an alumina scintillator and gated CCD camera after two solenoids has a hollow center (Fig. 7), a feature not seen in the measurements directly after the diode. The degradation of the scintillator light output as a function of ion beam fluence was quantified, and is not responsible for this observation. The hollow center, supported in slit profile scans, is not yet reproduced in simulations initialized at the emitter surface. There is a lower intensity region in the outer few mm of the beam, another feature not seen in the injected beam, and possibly a signature of incipient halo formation.

Intercepting diagnostics at the exit of the second solenoid, but still in its fringe field ($B_z \sim 1$ kG, depending on the diagnostic plane axial position) can cause a buildup of charge in the region a few centimeter upstream of the diagnostics. This is due to desorption of electrons and neutral atoms at the diagnostic surface, and subsequent ionization of the desorbed gas. Some features of the signal induced on a nearby biased electron suppressor are qualitatively reproduced by multi-species PIC simulations that self-consistently track the beam ions, desorbed electrons, gas and secondary ions and electrons [19]. This phenomenon gives rise to spurious results in the beam diagnostics—an apparent rapid time dependence of the envelope parameters. The problem is mitigated in the experiment by moving the diagnostics downstream by 29 cm, where the magnetic field is reduced by a factor ≈ 30. However, we are using this as an initial step toward modeling gas and electron effects in the presence of a solenoid field.

An axially moveable pepperpot-scintillator detector has been built to directly measure the beam transverse phase space within the solenoids. The beam would ideally rotate at the Larmor frequency of $\omega_{\text{Larmor}} \approx 1.7 \times 10^6$ rad/s, and the pepperpot measurement will give information about the evolution of the transverse phase space as a function of axial position.

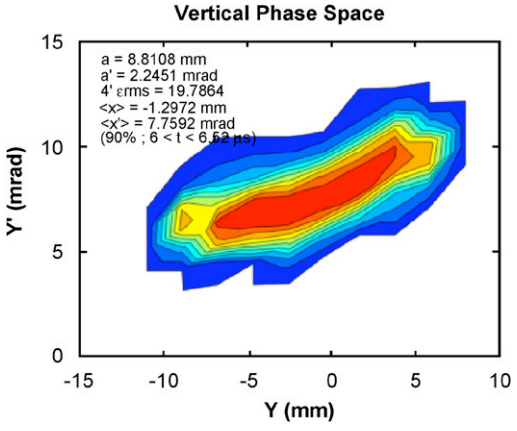

Fig. 6. Vertical phase space (y–y') of the beam transported through two solenoids.

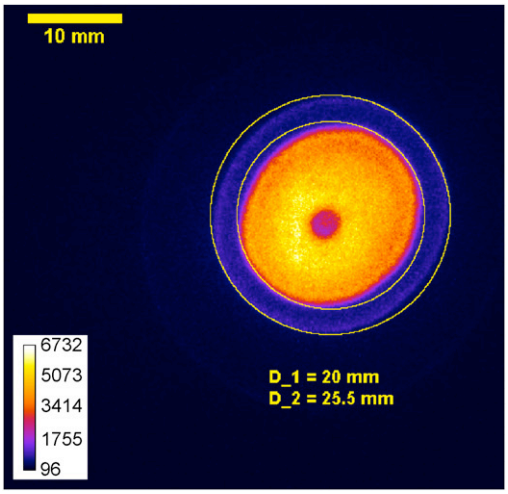

Fig. 7. Transverse current density distribution of the beam after two solenoids. The yellow circles indicate the approximate diameter (20 mm) of the core of the beam and a lower intensity region that extends to 25.5 mm.

To study and control electrons that may contribute to non-ideal beam transport and to beam quality degradation, short cylindrical electrodes with an inner diameter of 68 mm are inserted into the beam tube for the four-solenoid experiments [20]. These electron-cloud diagnostics can be biased up to 1 kV, and can be configured to collect electrons in the gaps between solenoids where magnetic field lines intercept the cylinders, or trap them in a Penning-like geometry to benchmark electron cloud simulation codes [21]. Note that the maximum beam envelope diameter in these experiments in the solenoids is 50–60 mm, filling a substantial fraction of the channel.

Analysis of the data for transport through four solenoids is underway.

6. Summary

This paper focuses on the plans and recent results of beam dynamics experiments toward the high-intensity conditions suitable for WDM studies. In order to provide the needed target energy density, all the components of such a facility have been, or will be tested in smaller scale beam experiments.

Acknowledgments

We are grateful for the excellent technical support of the mechanical and electrical teams led by Wayne Greenway and Craig Rogers.

This work was performed under the auspices of the U.S. Department of Energy by the University of California,

Lawrence Berkeley and Lawrence Livermore National Laboratories under contract numbers DE-AC02-05CH11231 and W-7405-Eng-48, and by the Princeton Plasma Physics Laboratory under contract number DE-AC02-76CH03073.

References

[1] B.G. Logan, et al., Nucl. Instr. and Meth. A (2007), doi:10.1016/j.nima.2007.02.070.
[2] F.M. Bieniosek, et al., Nucl. Instr. and Meth. A (2007), doi:10.1016/j.nima.2007.02.063.
[3] P.K. Roy, et al., Nucl. Instr. and Meth. A (2007), doi:10.1016/j.nima.2007.02.056.
[4] P.K. Roy, et al., Phys. Rev. Lett. 95 (2005) 234801.
[5] A.B. Sefkow, et al., Phys. Rev. ST-AB 9 (2006) 052801.
[6] P.K. Roy, et al., Nucl. Instr. and Meth. A 544 (2005) 255.
[7] A. Anders, G.Y. Yushkov, J. Appl. Phys. 91 (2002) 4824.
[8] P. Efthimion, et al., these proceedings.
[9] R.J. Briggs, Phys. Rev. ST Accel. Beams 9 (2006) 060401.
[10] P.K. Roy, et al., Phys. Rev. ST Accel. Beams 9 (2006) 070402.
[11] J.E. Coleman, et al., Nucl. Instr. and Meth. A (2007), doi:10.1016/j.nima.2007.02.053.
[12] A. Friedman, Nucl. Instr. and Meth. A (2007), doi:10.1016/j.nima.2007.02.010.
[13] C.H. Thoma, et al., Proceedings of the 2005 Particle Accelerator Conference, IEEE, Piscataway, NJ 08855-1331 USA. p. 4006.
[14] D.R. Welch, et al., Nucl. Instr. and Meth. A (2007), doi:10.1016/j.nima.2007.02.057.
[15] A.B. Sefkow, et al., Nucl. Instr. and Meth. A (2007), doi:10.1016/j.nima.2007.02.064.
[16] M. Reiser, Theory and Design of Charged Particle Beams, Wiley, New York, 1994.
[17] L.R. Prost, et al., Phys. Rev. ST Accel. Beams 8 (2005) 020101.
[18] A. Friedman, et al., Proceedings of the 2003 Particle Accelerator Conference, IEEE, Piscataway, NJ, USA. p. 275.
[19] W.M. Sharp, et al., Nucl. Instr. and Meth. A (2007), doi:10.1016/j.nima.2007.02.046.
[20] A.W. Molvik, et al., these proceedings.
[21] J.-L. Vay, et al., Nucl. Instr. and Meth. A (2007), doi:10.1016/j.nima.2007.02.013.